Electronic Supplementary Material (ESI) for Nanoscale.

Electronic Supplementary Information (ESI)

Radial ZnO Nanorods Decorating Co_3O_4 Nanoparticles for Highly Selective and Sensitive Detection of 3-Hydroxy-2-Butanone Biomarker

Chen Wang, Lingling Du, Xiaxia Xing, Dongliang Feng, Yingying Tian, Zhenxu Li, Xinhua Zhao and Dachi Yang*

Tianjin Key Laboratory of Optoelectronic Sensor and Sensing Network Technology, Department of Electronics, College of Electronic Information and Optical Engineering, Nankai University, Tianjin 300350, China

E-mail: yangdachi@nankai.edu.cn

Outline

Experimental section

Synthesis of ZnO NRs / Co_3O_4 NPs

The optimal ZnO NRs / Co_3O_4 NPs were prepared through a facile hydrothermal process and post annealing treatment.[1] Firstly, 0.073 g cetyltrimethylammonium bromide (CTAB) and 1.92 g NaOH were dissolved into 20 mL deionized water under magnetic stirring. Subsequently, 2.32 g $Zn(NO_3)_2 \cdot 6H_2O$ and 0.2838g $Co(NO_3)_2 \cdot 6H_2O$ were dissolved into 20 mL deionized water to obtain Zn / Co molar ratio of 8, and the obtained mixture was added dropwise to above alkaline aqueous solution. In the dripping process, the color of the solution changed from colorless to deep blue and finally to pink, and the viscosity increased gradually. After another 30 min vigorous stirring, the mixture was then transferred into a Teflon-lined stainless-steel autoclave and maintained the temperature at 95 °C for 10 h. Afterwards, the precipitate was filtered, rinsed with deionized water and ethanol, dried at 60 ^oC for 6 h. Finally, the glaucous product was obtained by annealing the as-prepared powder in air atmosphere at 300 °C for 12 h with a ramping rate of 2 $^oC \cdot min^{-1}$. For comparison, pure ZnO nanorods (NRs), pure Co_3O_4 nanoparticles (NPs) and ZnO NRs / Co_3O_4 NPs with various Zn / Co molar ratios of 2, 4 and 16 were prepared using the same procedure by modulating the additive amount of $Co(NO_3)_2 \cdot 6H_2O$. The samples with various Zn / Co molar ratios were denoted as ZnO NRs / Co_3O_4 NPs -2, ZnO NRs / Co_3O_4 NPs -4, ZnO NRs / Co_3O_4 NPs -8 and ZnO NRs / Co_3O_4 NPs -16, respectively.

Characterizations

The morphology and crystalline structure were characterized by field emission scanning electron microscope (FE-SEM, JSM-7800F) with an energy dispersive X-ray spectrometer

(EDS, Oxford), transmission electron microscopy (TEM, JEM-2800) with high-resolution TEM (HRTEM) and X-ray diffraction (XRD, Rigaku SmartLab, 3 KW). X-ray photoelectron spectroscopy (XPS, Thermo Scientific ESCALAB 250Xi) was applied to investigate surface elemental information of the samples. Ultraviolet-visible (UV-vis) absorption spectrum (TU-1901 UV-vis spectrophotometer) was conducted to deduce band structure. Mott-Schottky and electrochemical impedance spectroscopy (EIS) measurements were performed on electrochemical workgroup (VersaSTAT 4, AMETEK Princeton) with a standard three-electrode configuration, wherein the electrolyte is 0.2 M Na_2SO_4 aqueous solution (pH = 6.5).

The sensing evaluations

The fabrication of the sensor prototypes was similar to our previous research.[2-4] The gas-sensing test was conducted on the WS-30B test system (Weisheng Instruments Co., Zhengzhou, China) at a relative humidity of 15%-30%. The response of all the sensors is defined as $S = R_a / R_g$ except for the Co_3O_4 NPs sensor ($S = R_g / R_a$), where R_a and R_g are the resistance in air and target gas ambient, respectively. The response and recovery time are designated as the time taken for the sensor to reach 90% response variation of its saturation state after the injection or release of target gas.

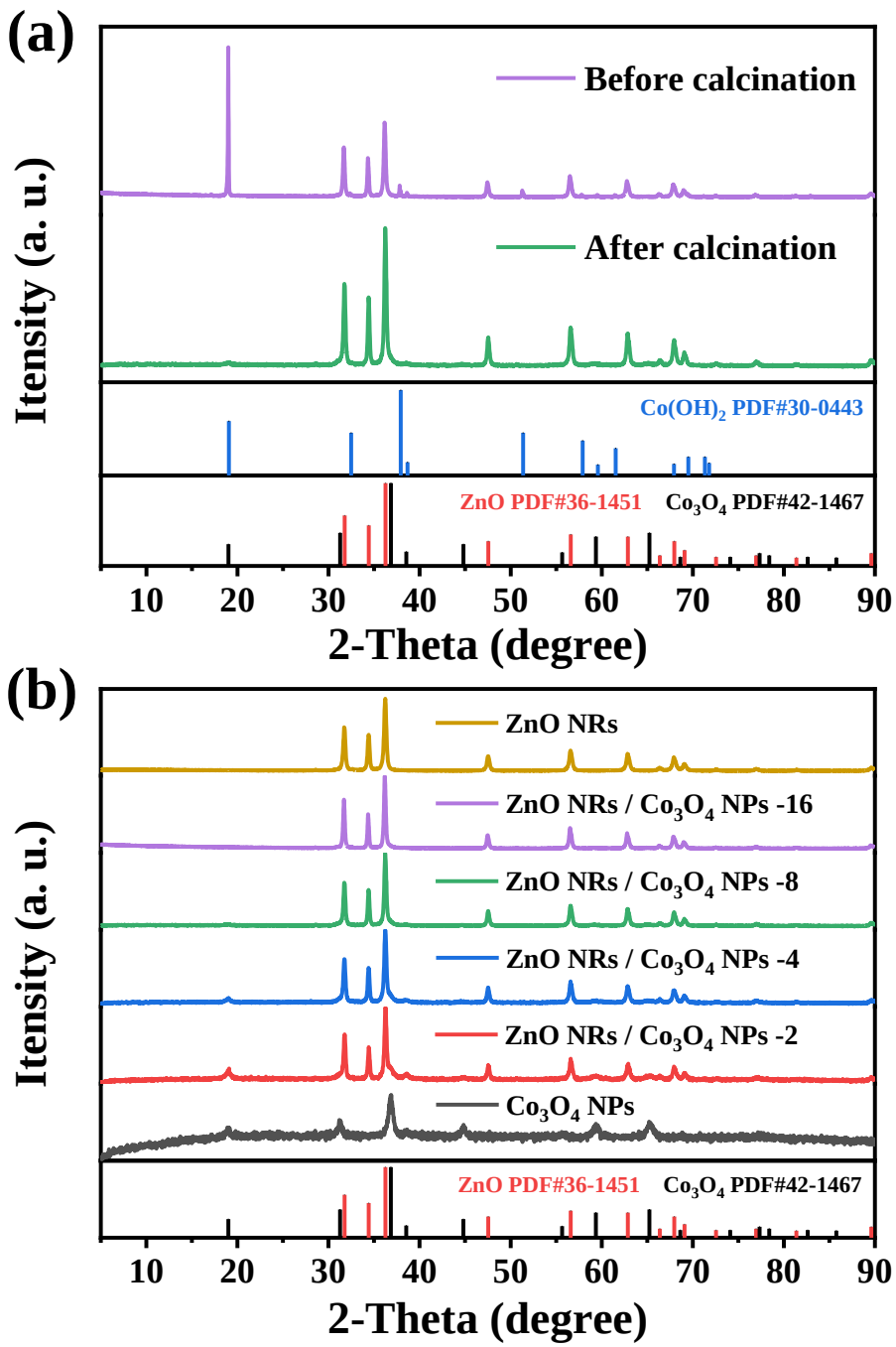

Fig. S1 (a) XRD patterns of ZnO NRs / Co_3O_4 NPs -8 before and after calcination. (b) XRD patterns of ZnO NRs / Co_3O_4 NPs with various Zn / Co molar ratios.

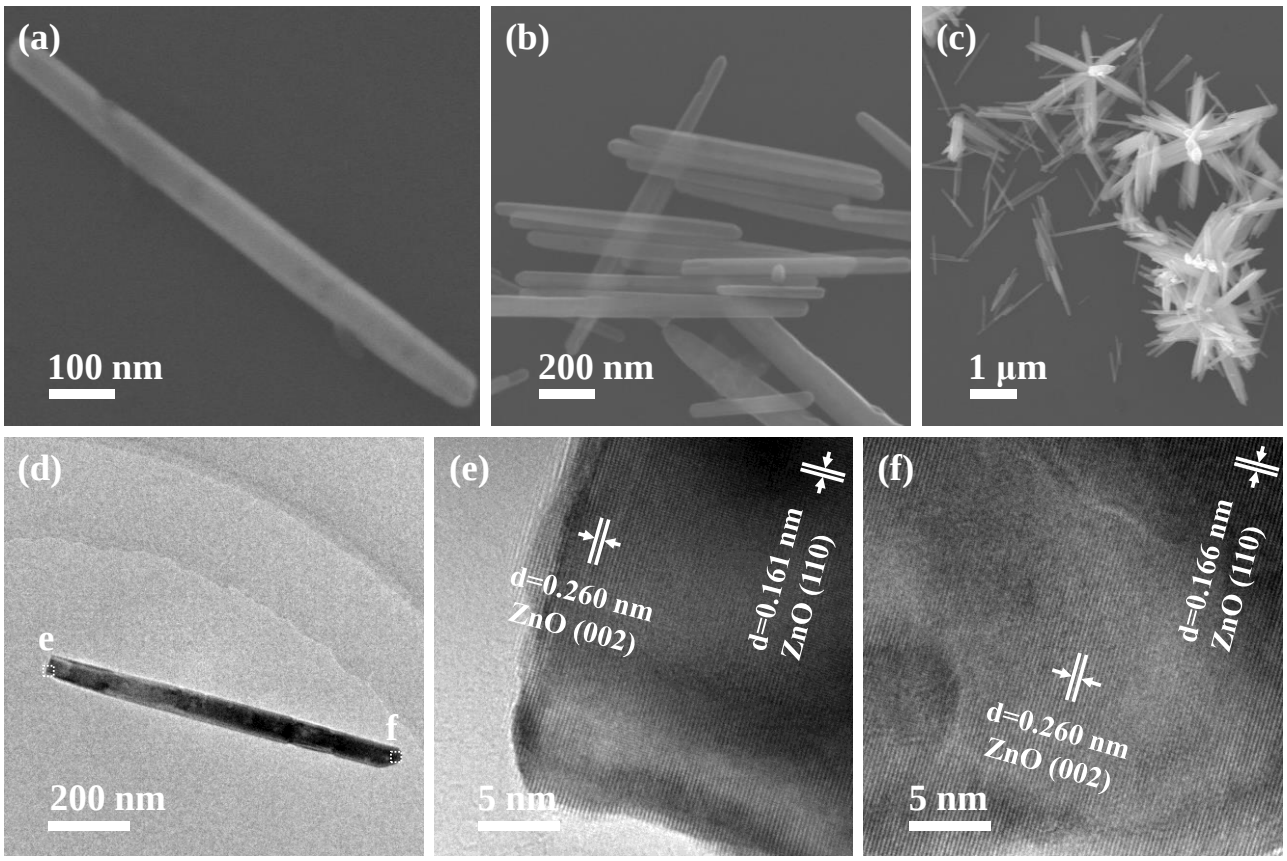

Fig. S2 (a-c) SEM images of ZnO NRs. (d) TEM image of individual ZnO NRs. (e-f) HRTEM images taken from the dashed rectangle in (d).

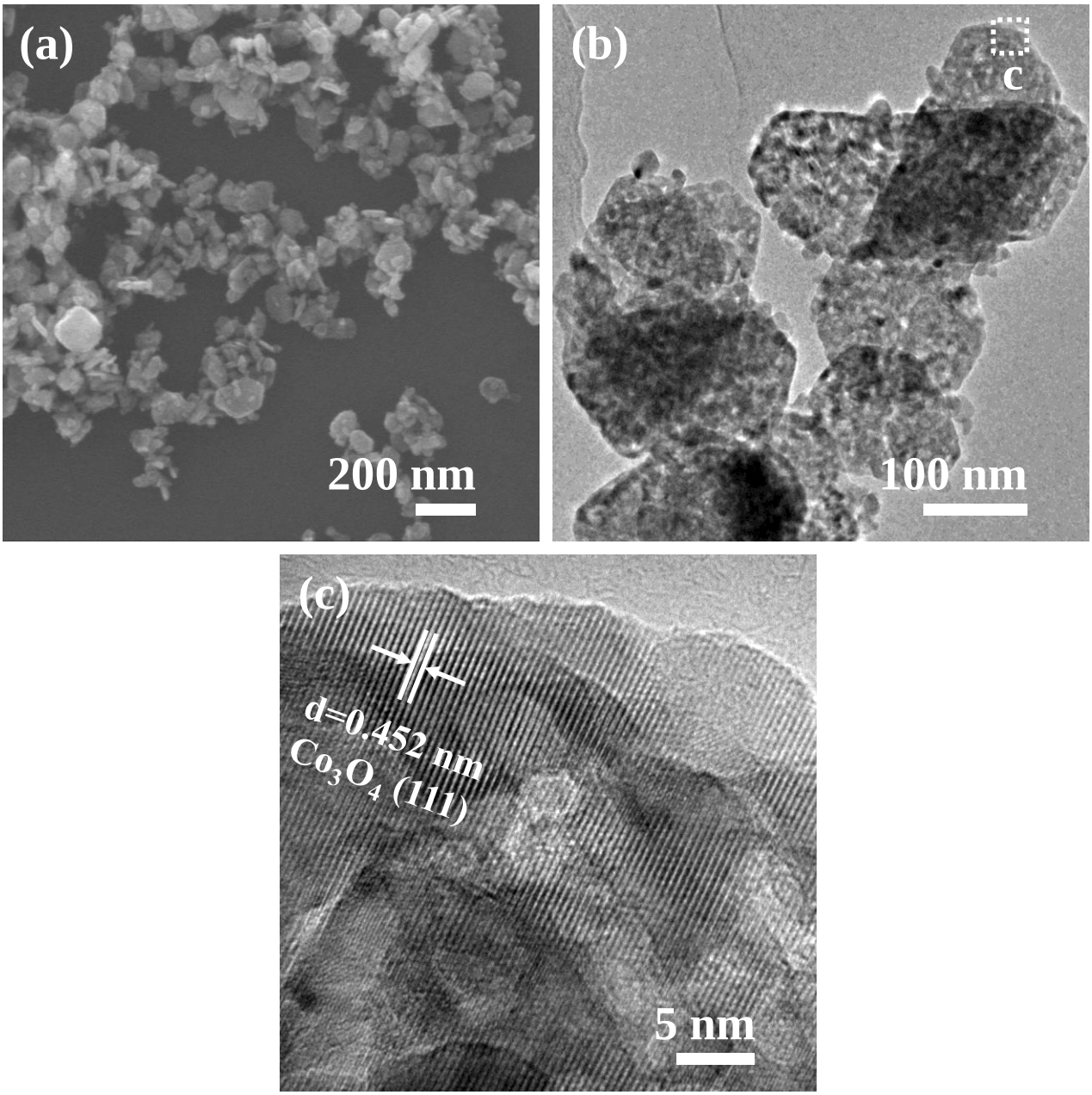

Fig. S3 (a) SEM and (b) TEM images of Co_3O_4 NPs. (c) HRTEM image taken from the dashed rectangle in (b).

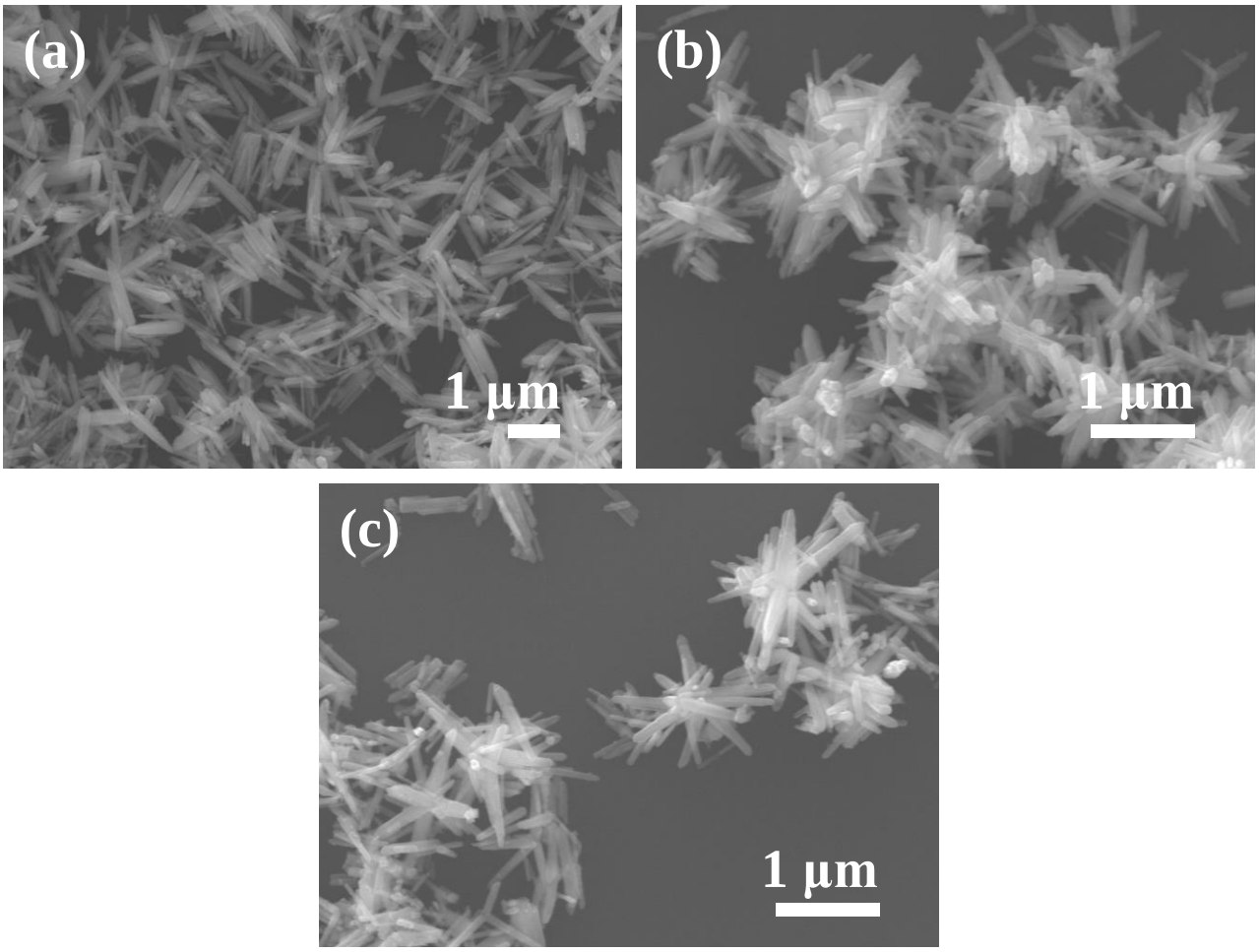

Fig. S4 SEM images of (a) ZnO NRs / Co_3O_4 NPs -16, (b) ZnO NRs / Co_3O_4 NPs -4 and (c) ZnO NRs / Co_3O_4 NPs -2.

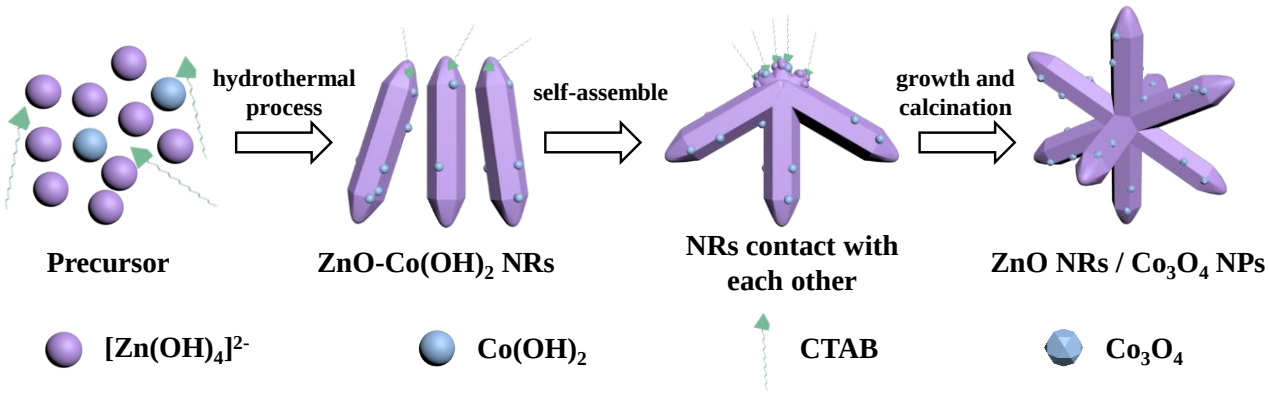

Scheme S1 Schematic synthesis of ZnO NRs / Co_3O_4 NPs.

The proposed formation process of the ZnO NRs / Co_3O_4 NPs are described in Scheme S1 †.

$$Zn^{2+}+OH^{-}\leftrightarrow Zn(OH)_2 \quad (1)$$

$$Zn(OH)_2+2OH^{-}\leftrightarrow [Zn(OH)_4]^{2-} \quad (2)$$

$$CTAB\leftrightarrow CTA^{+}+Br^{-} \quad (3)$$

$$[Zn(OH)_4]^{2-}+CTA^{+}\leftrightarrow CTA^{+}\text{-}[Zn(OH)_4]^{2-} \quad (4)$$

$$Zn(OH)_2\leftrightarrow ZnO+H_2O \quad (5)$$

$$CTA^{+}\text{-}[Zn(OH)_4]^{2-}\leftrightarrow ZnO+H_2O+CTA^{+} \quad (6)$$

$$Co(NO_3)_2\cdot 6H_2O+2NaOH\rightarrow Co(OH)_2+2NaNO_3+6H_2O \quad (7)$$

$$3Co(OH)_2+\frac{1}{2}O_2\rightarrow Co_3O_4+3H_2O \quad (8)$$

In weakly basic solution, $Zn(OH)_2$ precipitation is partially dissolved in the form of $[Zn(OH)_4]^{2-}$ (equation 2).[5] Surfactant CTAB not only reduces the surface tension of solution and the energy required to form a new phase, but also acts as ionic compound, ionizing CTA^{+}, negatively charging $[Zn(OH)_4]^{2-}$ to form CTA^{+}-$[Zn(OH)_4]^{2-}$ through electrostatic interaction, and accelerating the orientation growth of ZnO NRs (equation 3, 4).[1] Moreover, the another

precursor $Co(NO_3)_2 \cdot 6H_2O$ combines with abundant OH^- to generate $Co(OH)_2$ NPs attached to ZnO NRs (equation 7). Then, as the ZnO-$Co(OH)_2$ NRs have grown long enough, some of them begin to be tilted and contact with each other and be coalesced.[6] On account of Co ion has a higher electronegativity (1.88) than Zn ion (1.65), this might lead to the formation of dipole that facilitates the NRs contacting and combining together to form new nucleation points, which is verified by Fig. S4†.[7] Finally, the growth units aggregate at the new nucleation point and grow axially, resulting to the formation of ZnO NRs / Co_3O_4 NPs after calcination.

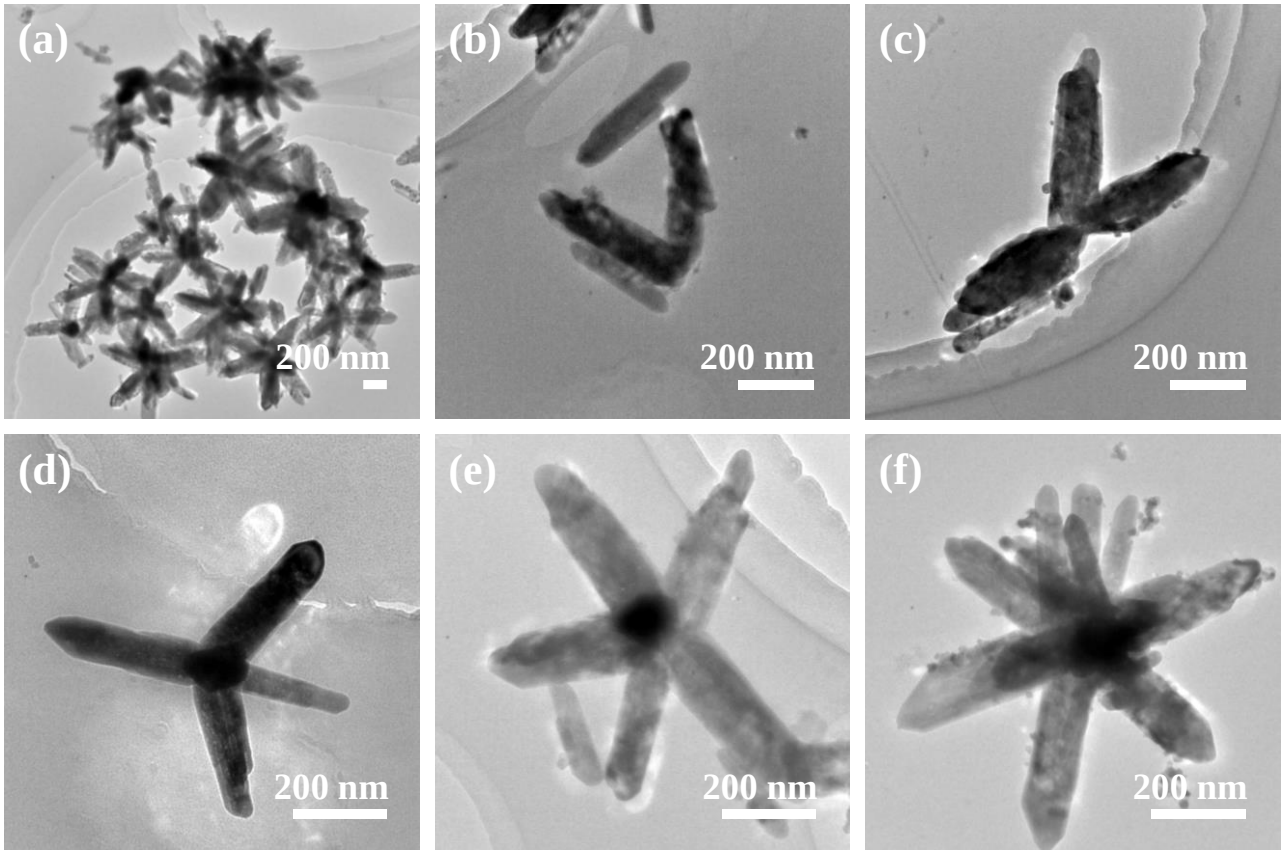

Fig. S5 (a-f) TEM images of ZnO NRs / Co_3O_4 NPs with varying amounts of NRs.

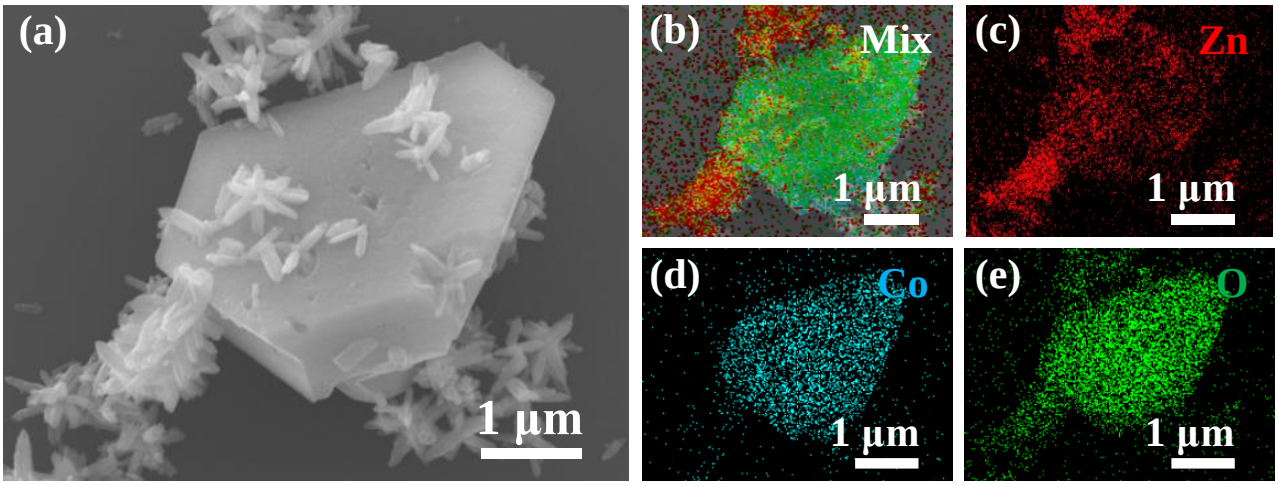

Fig. S6 (a) SEM image. (b-e) EDS mappings of ZnO NRs / Co_3O_4 NPs.

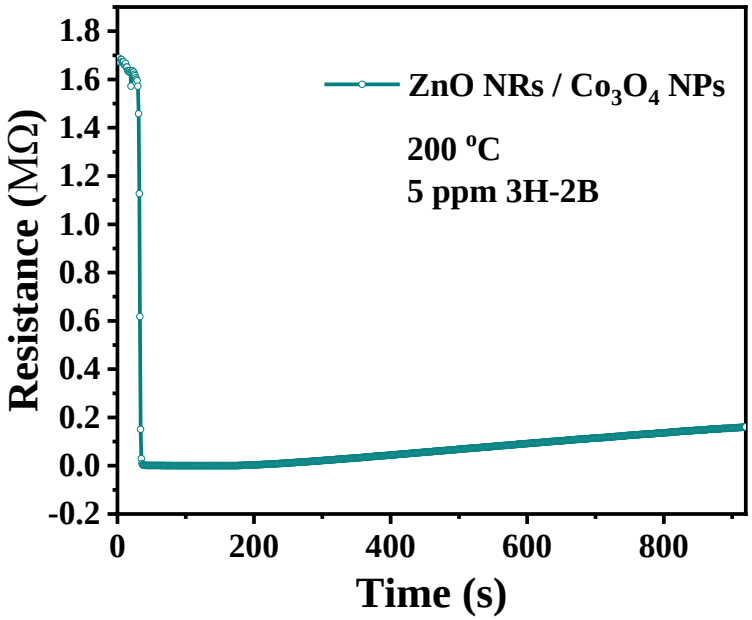

Fig. S7 The resistance variation of ZnO NRs / Co_3O_4 NPs to 5 ppm 3H-2B at 200 °C.

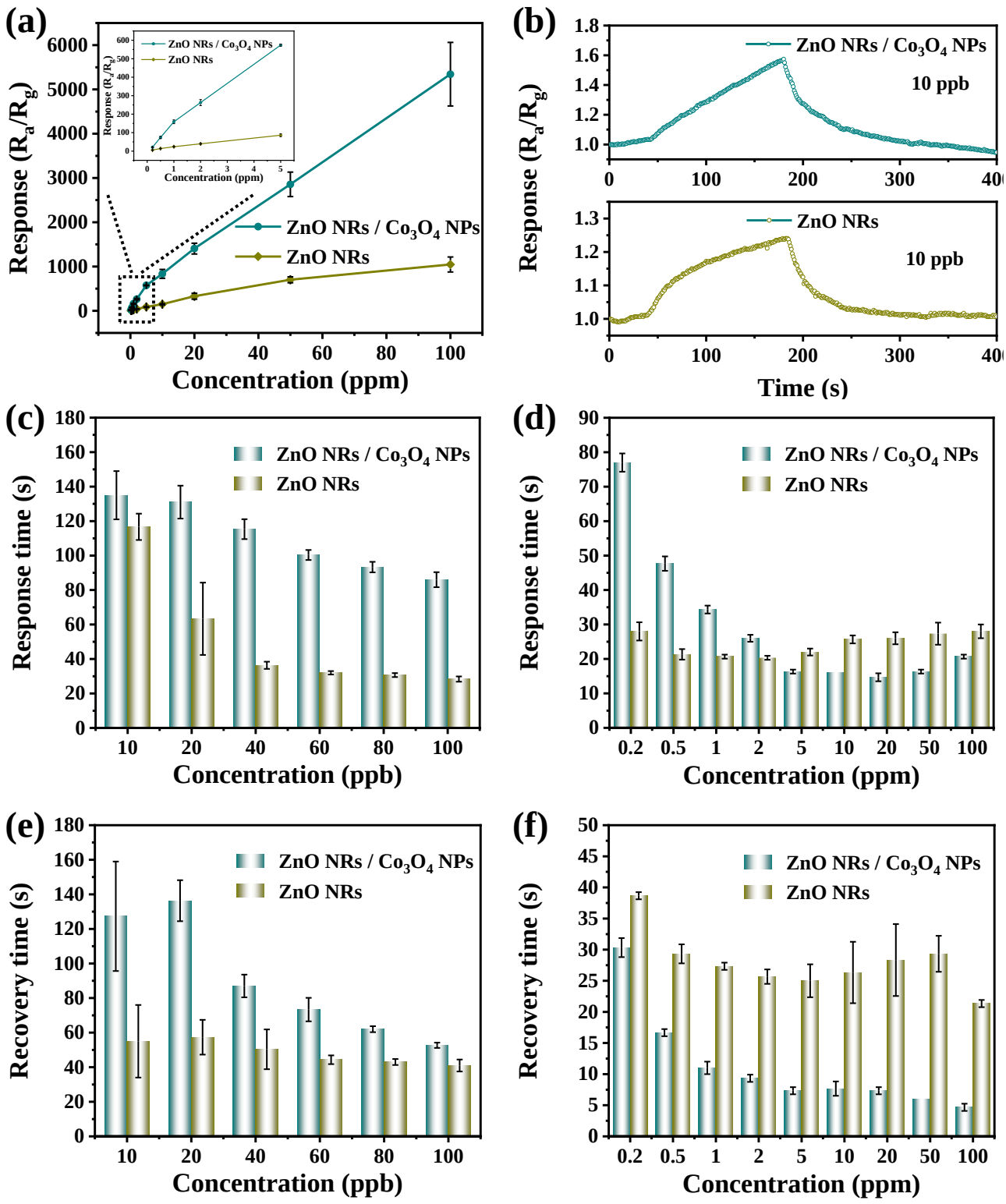

Fig. S8 (a) The summarized response of ZnO NRs / Co_3O_4 NPs and ZnO NRs toward 100 ppb-100 ppm at 260 °C. (b) The response of ZnO NRs / Co_3O_4 NPs and ZnO NRs toward 10 ppb 3H-2B at 260 °C. (c-d) The response time and (e-f) recovery time of ZnO NRs / Co_3O_4 NPs and ZnO NRs toward 10 ppb-100 ppm 3H-2B at 260 °C.

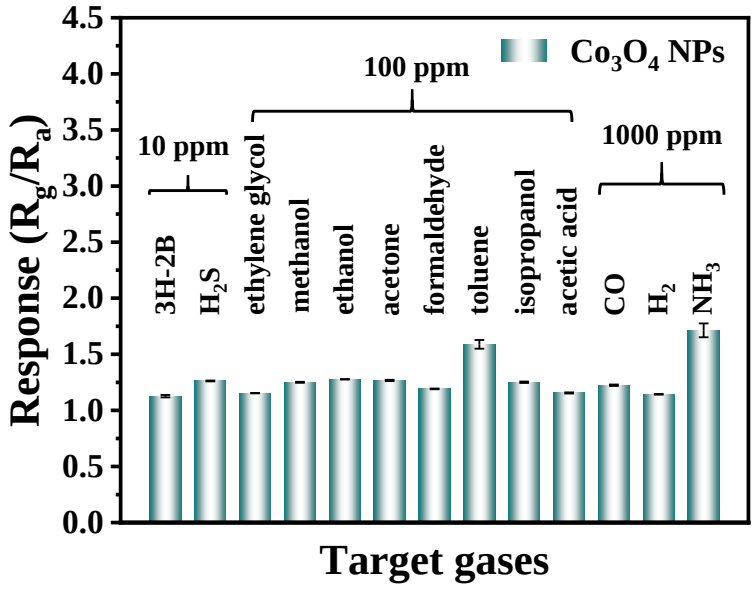

Fig. S9 The selectivity of the Co_3O_4 NPs toward 10 ppm 3H-2B and interfering gases at 260 ^oC.

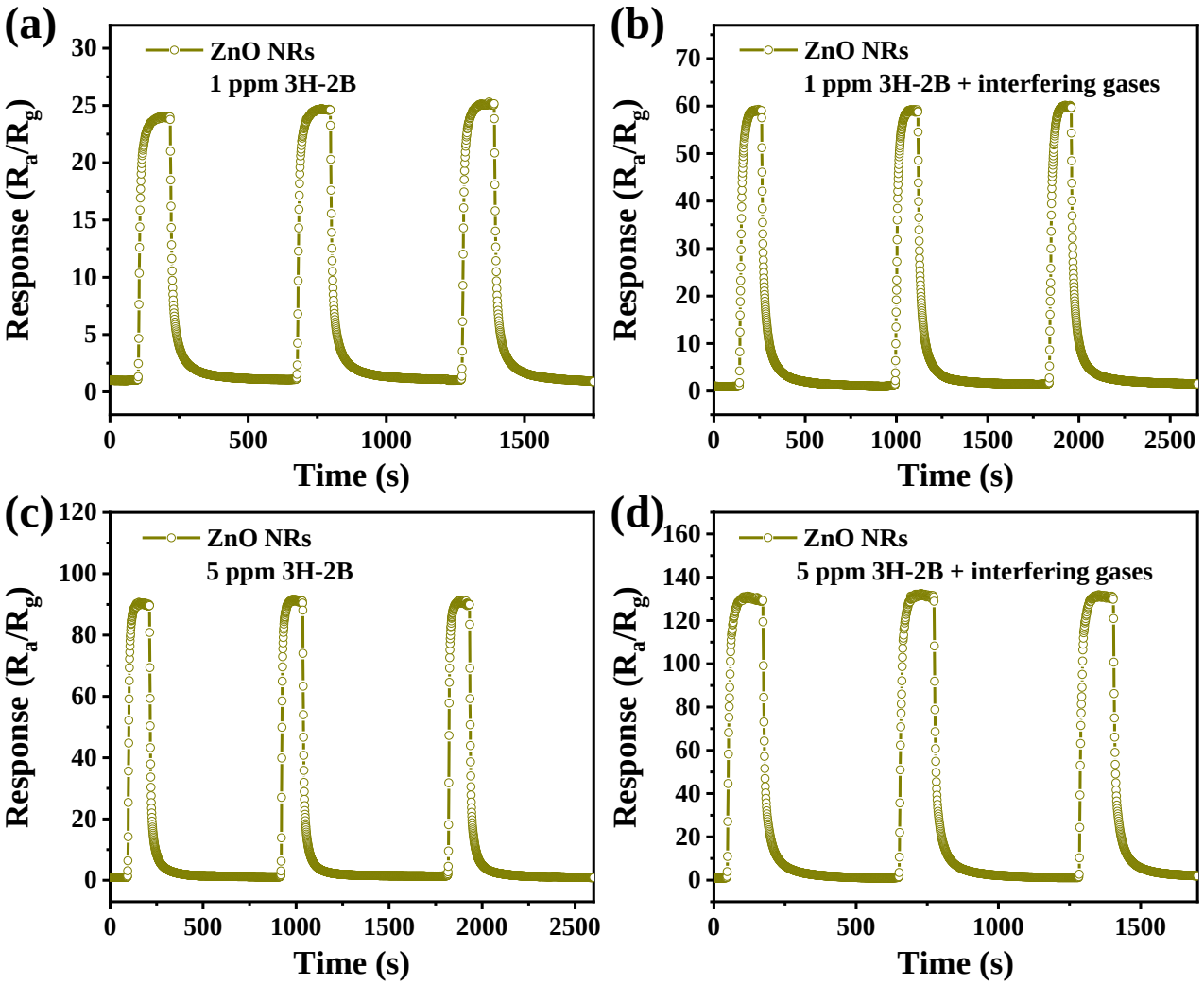

Fig. S10 Response of ZnO NRs to (a) 1 ppm 3H-2B, (b) 1 ppm 3H-2B + interfering gases, (c) 5 ppm 3H-2B, and (d) 5 ppm 3H-2B + interfering gases. Interfering gases in (b) and (d) include ethylene glycol with same concentration as 3H-2B, as well as methanol, ethanol, acetone, formaldehyde, toluene, isopropanol and acetic acid, of which the concentrations are applied ten times than that of 3H-2B.

Table S1 Features of ZnO NRs / Co_3O_4 NPs sensor toward 1 ppm various gases for the principal component analysis (PCA). (Notation: R: Response. t_{Res}, t_{Rec}: Response time, Recovery time. $R_{@10, 20, 30\ s}$: Response at 10, 20, 30 s. Max. dR_{ads}/dt: Maximum slope of the response from the transient curves).

Gas	R	t_{Res}	t_{Rec}	$R_{@10s}$	$R_{@20s}$	$R_{@30s}$	Max. dR_{ads}/dt (s^{-1})
3H-2B	157.2	33	11	66.51	117.48	136.52	10.6048
3H-2B	169.43	35	10	74.69	125.87	147.74	8.8411
Benzaldehyde	7.61	199	185	1.53	2.19	2.57	0.0833
Benzaldehyde	7.26	200	188	1.22	1.85	2.44	0.0625
2, 3-butanedione	10.14	105	153	2.2	3.86	5.1	0.1648
2, 3-butanedione	10.89	96	152	2.74	4.52	5.85	0.1807
2, 5-dimethyl-pyrazine	7.44	176	341	1.67	2.35	2.96	0.0698
2, 5-dimethyl-pyrazine	7.24	190	343	1.72	2.35	2.91	0.0595
3-methybutanal	8.97	137	170	1.63	2.74	3.72	0.1031
3-methybutanal	8.96	130	168	2.27	3.15	4.03	0.1071

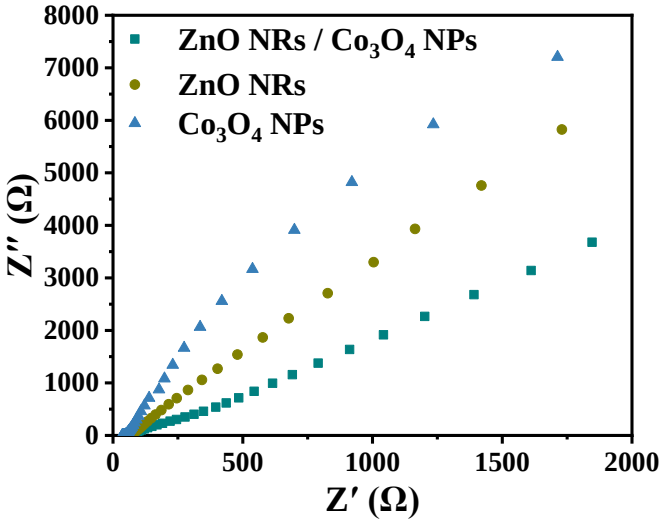

Fig. S11 Nyquist plots of ZnO NRs / Co_3O_4 NPs, ZnO NRs and Co_3O_4 NPs.

Table S2 Comparison of the sensing performance of MOS-based sensors for 3H-2B biomarker detection.[2, 3, 8-14]

Sensing materials	Gas concentration (ppm)	Working temperature (^oC)	Response (R_a/R_g)	Detection limit	Response/ Recovery time	References
Mesoporous WO_3	5	290	27	0.1 ppm	4 s/13 s	[8]
Cr/WO_3 nanofibers	5	140	71.8	0.05 ppm	27 s/36 s	[2]
Mesoporous NiO nanocuboids	50	120	302	0.5 ppm	92 s/82 s	[3]
ZnO@Al_2O_3 nanocables	50	300	37.2	1 ppm	27 s/34 s	[9]
Pt/SnO_2 hollow nanospheres	10	250	48.69	0.5 ppm	11 s/20 s	[10]
SnO_2@Al_2O_3 nanocables	5	120	43.3	0.1 ppm	48 s/194 s (0.5 ppm)	[11]
PtCu/WO_3 hollow sphere	10	110	221.2	0.5 ppm	9 s/28 s	[12]
Mesoporous WO_3 nanoflowers	25	205	152	0.4 ppm	25 s/146 s	[13]
Pd-{010}$BiVO_4$ microdecahedrons	10	200	103.7	0.2 ppm	12 s/8 s	[14]
ZnO NRs / Co_3O_4 NPs	**5**	**260**	**550**	**10 ppb**	**17 s/8 s**	**This work**

References

1 L. Wang, Y. Kang, X. Liu, S. Zhang, W. Huang and S. Wang, *Sens. Actuators, B*, 2012, **162**, 237-243.

2 Z. Zhu, L. Zheng, S. Zheng, J. Chen, M. Liang, Y. Tian and D. Yang, *J. Mater. Chem. A*, 2018, **6**, 21419-21427.

3 Z. Zhu, L. Zheng, S. Zheng, J. Chen, X. Xing, D. Feng and D. Yang, *J. Mater. Chem. A*, 2019, **7**, 10456-10463.

4 D. Feng, L. Du, X. Xing, C. Wang, J. Chen, Z. Zhu, Y. Tian and D. Yang, *ACS Sens.*, 2021, **6**, 733-741.

5 B. G. Wang, E. W. Shi and W. Z. Zhong, *Cryst. Res. Technol.*, 1997, **32**, 659-667.

6 J.-M. Jang, C.-R. Kim, H. Ryu, M. Razeghi and W.-G. Jung, *J. Alloys Compd.*, 2008, **463**, 503-510.

7 P. Rai, J.-N. Jo, I.-H. Lee and Y.-T. Yu, *Mater. Chem. Phys.*, 2010, **124**, 406-412.

8 Y. Zhu, Y. Zhao, J. Ma, X. Cheng, J. Xie, P. Xu, H. Liu, H. Liu, H. Zhang, M. Wu, A. A. Elzatahry, A. Alghamdi, Y. Deng and D. Zhao, *J. Am. Chem. Soc.*, 2017, **139**, 10365-10373.

9 J. Chen, Z. Zhu, S. Zheng, L. Du, X. Xing, D. Feng, S. Li and D. Yang, *Mater. Lett.*, 2019, **253**, 121-123.

10 H. Cai, H. Liu, T. Ni, Y. Pan, Y. Zhao and Y. Zhu, *Front. Chem.*, 2019, **7**, 843.

11 X. Xing, Z. Zhu, L. Du, D. Feng, J. Chen, S. Li and D. Yang, *Appl. Surf. Sci.*, 2020, **502**, 144106.

12 D. Wang, L. Deng, H. Cai, J. Yang, L. Bao, Y. Zhu and X. Wang, *ACS Appl. Mater. Interfaces*, 2020, **12**, 18904-18912.

13 D. Xu, K. Ge, S. Qi, Y. Chen, J. Qiu and Q. Liu, *Anal. Bioanal. Chem.*, 2020, **412**, 8371-8378.

14 J. Chen, D. Feng, C. Wang, X. Xing, L. Du, Z. Zhu, X. Huang and D. Yang, *ACS Sens.*, 2020, **5**, 2620-2627.